Mussel larval responses to turbulence are unaltered by larvalage or light condition

Limnology and Oceanography
FLUIDS & ENVIRONMENTS

ORIGINAL ARTICLE

Mussel larval responses to turbulence are unaltered by larval age or light conditions

Heidi L. Fuchs[1] **and Claudio DiBacco**[2]

Abstract

*Larval responses to hydromechanical cues potentially have important effects on larval dispersal and settlement. This study examined the behavior of mussel larvae (*Mytilus edulis*) in laboratory-generated turbulence representative of nearshore currents. We video recorded the behavior of early- and late-stage veligers in a grid-stirred tank at five turbulence levels under light and dark conditions. Water velocities and kinetic energy dissipation rates were measured using particle image velocimetry and acoustic Doppler velocimetry. We characterized the vertical velocity distributions for sinking, hovering, and swimming modes in still water and calculated the average larval behavioral velocity in turbulence. In still water, young larvae had more positive (upward) velocities than old larvae, and both stages had more positive velocities in light than in dark. In turbulence, the mean larval vertical velocity varied from positive at low dissipation rates to negative at dissipation rates above a threshold of 8.3×10^{-2} cm^2 s^{-3}. At this threshold, the Kolmogorov length scale ($\eta = 590$ μm) was two to three times the mean larval shell lengths (171–256 μm), implying that turbulence is detectable even by larvae that are smaller than the smallest eddies. Responses to turbulence were unaffected by larval age or light conditions and contributed substantial behavioral variation. By sinking in strong turbulence, mussel larvae could increase their flux to the bed in energetic coastal flows, particularly over rough substrates like mussel beds. The response to turbulence by early-stage larvae will also affect their dispersal and may help larvae remain near coastal populations.*

Keywords: dispersal, larval behavior, *Mytilus edulis*, ontogeny, settlement

Introduction

[1] Some mollusk larvae (veligers) stop swimming and sink in strong turbulence (e.g., Barile et al. 1994; Young 1995), potentially as an adaptation to disperse and settle more successfully in energetic coastal regions. For example, larvae of intertidal mud snails (*Ilyanassa obsoleta*) pull in their velum and sink more frequently in turbulence above a kinetic energy dissipation rate of $\varepsilon \approx 4.0 \times 10^{-1}$ cm^2 s^{-3} (i.e., 4.0×10^{-5} m^2 s^{-3}; centimeter units are more relevant to larval scales; Fuchs et al. 2004). Conversely, the larvae of snails (*Crepidula* spp. and *Anachis* spp.) from shallow subtidal beaches sink in calmer water and swim upward in turbulence above a threshold level (Fuchs et al. 2010). These genus-specific responses to turbulence suggest that behavior plays a different role in larval transport for species from different habitat types. Bivalve veligers may also have flow-mediated behaviors that affect their dispersal and settlement, but quantitative

[1]Institute of Marine and Coastal Sciences, Rutgers University, New Brunswick, New Jersey 08901, USA

[2]Bedford Institute of Oceanography, Fisheries and Oceans Canada, Dartmouth, Nova Scotia B3B 1A5, Canada

Correspondence to
Heidi L. Fuchs
hfuchs@marine.rutgers.edu

observations are lacking. Although oyster larvae "dive-bomb" by suddenly accelerating downward in flume flow (Finelli and Wethey 2003), the cue for sinking is undocumented. Further study is needed to determine if bivalve larvae respond to turbulence.

[2] Blue mussel *Mytilus edulis* (Linnaeus) larvae are of interest because they recruit into varied coastal habitat types and the adults live in diverse habitat types and flow regimes. *M. edulis* attach to filamentous or hard substrates, including adult mussels, in coastal habitats ranging from rocky shores to muddy inlets (e.g., Bayne 1964a; Suchanek 1978; Petersen 1984). Turbulence may provide a behavior cue for mussel larvae by broadly indicating proximity to shore. In tidal channels and estuaries, for example, dissipation rates reach approximately 1 to 10 $cm^2 s^{-3}$ (Gross and Nowell 1985; Peters 1997), whereas in oceanic mixed layers they are typically $< 0.01\ cm^2 s^{-3}$ (Dillon and Caldwell 1980; Oakey and Elliott 1982). Increased water flow enhances settlement of *Mytilus* larvae in laboratory experiments, but this effect is partly due to the increased flux of larvae to surfaces in stronger turbulence (Eyster and Pechenik 1988; Eckman and Duggins 1998), and it remains unclear whether turbulence affects larval behavior. Larvae that sink in turbulence could concentrate lower in the water column in more energetic coastal waters, improving their chances of being retained and settling in shallow nearshore habitats (e.g., Fuchs et al. 2007).

[3] Compared to snail larvae studied previously, mussel larvae may react to stronger turbulence if their smaller size makes turbulence more difficult to detect. The length scale of the smallest eddies (Kolmogorov scale) is defined by the dissipation rate ε and the kinematic viscosity ν as $\eta = (\nu^3/\varepsilon)^{0.25}$. Snail larvae change their behavior when η is on the order of the larval length scale; larvae in the laboratory switched from swimming to sinking at $\eta \approx 400\ \mu m$, or about half the larval length including the velum (Fuchs et al. 2004), whereas larvae in the field changed their behavior at $\eta \approx 560–800\ \mu m$, roughly equivalent to the larval size range (Fuchs et al. 2010). This limited evidence suggests that sensitivity to turbulence may involve interactions between larvae and eddies of similar size, for example, by larvae detecting differences in shear across the length of the velum. Bivalve larvae are smaller than snail larvae at settlement (approx. 200 to 300 μm), and an equivalent Kolmogorov scale would be associated with relatively high dissipation rates of $\varepsilon = 1.3–6.3\ cm^2 s^{-3}$. We expect that the smaller bivalve larvae would change their behaviors at higher turbulence thresholds relative to snail larvae.

[4] Mussel larval behavior is also affected by gravity and light, but the direction of swimming and the magnitude of response vary widely with temperature and larval age (Bayne 1964b). Mussel larvae in the field are concentrated higher in the water column at night (Raby et al. 1994), suggesting that behavior may be partially governed by negative phototaxis combined with negative geotaxis. Observed vertical distributions are similar for both small and large larvae (Dobretsov and Miron 2001; Knights et al. 2006), which raises questions about age-related behavioral differences observed in the laboratory (Bayne 1964b). If behavior depends on a hierarchy of cues (Kingsford et al. 2002; Woodson et al. 2007), field environments may provide additional signals that overrule the behaviors observed under relatively artificial laboratory conditions.

[5] The goals of this study were to characterize behavior of mussel larvae in laboratory-generated turbulence and to test whether that behavior varied with larval age or light. We exposed early- and late-stage larvae to a range of turbulence representative of coastal currents and repeated the experiments in light and dark. We hypothesized that larvae would undergo ontogenetic changes in the response to light as observed by Bayne (1964b) and that larvae would sink more in turbulence above a threshold dissipation rate at which the Kolmogorov length scale was similar to the larval length scale.

Methods

Mussel Larvae

[6] Mussel larvae were spawned from preconditioned adults (*M. edulis*) and reared at 15 ± 1 °C at the Darling Marine Center (Walpole, ME, USA) in May 2008. Experiments were run with 10- to 13-day-old veliconcha larvae and 20- to 22-day-old eyed veligers, referred to hereafter as "young" and "old" larvae, respectively. Young larvae had mean ± SD lengths of 171 ± 8.6 μm on 10 May to 188 ± 15.5 μm on 13 May, and old larvae

had mean lengths of 243 ± 16.5 μm on 20 May to 256 ± 19.4 μm on 22 May. Before each set of experiments, approximately 5×10^5 larvae were transported in coolers to the shore lab at Woods Hole Oceanographic Institution (Woods Hole, MA, USA). Larvae were kept in 10-L buckets of 1- μm filtered seawater with continuous aeration and fed 5×10^4 cells mL^{-1} of *Isochrysis galbana* daily. Water in the cultures was changed every other day. Cultures were maintained at 15 ± 1 °C in a temperature-controlled room where experiments were performed.

Turbulence

[7] Behavioral experiments were run in an approximately 170-L tank with turbulence generated by two parallel stirring grids (Fig. 1). Grid-stirred turbulence is relatively homogeneous (statistically invariant in space) in planes parallel to the grid, stationary (statistically invariant in time), and nearly isotropic (statistically similar on each axis). Turbulence characteristics depend on the grid mesh size M, the oscillation amplitude S, the oscillation frequency f, and the distance from the grid z (Hopfinger and Toly 1976; Brumley and Jirka 1987). When two grids are used, turbulence is additive and symmetric between the grids, with a homogeneous region whose size depends on M and the distance between the grids H (Villermaux et al. 1995; Shy et al. 1997). For the larval experiments we used a single tank configuration with a grid spacing of $H = 45.7$ cm, a mesh size of $M = 6.35$ cm, and an oscillation amplitude of $S = 8.89$ cm. Flows were characterized for stirring frequencies of $f = 0.14–1.45$ Hz, and 1.20 Hz was the highest frequency used in larval experiments. Observations were centered at $z = 22.86$ cm from either grid.

[8] Prior to the behavior experiments, we characterized the turbulence in the center of the tank using particle image velocimetry (PIV) and acoustic Doppler velocimetry (ADV). The PIV included a 532 nm, dual-head, pulsed YAG laser (Big Sky Laser Technologies, USA) and a four-megapixel camera (LaVision, Germany) with a 50-mm lens (Nikon, Japan). The ADV was a 10-MHz ADVOcean (Sontek, USA). We seeded the tank with 20-μm hollow glass spheres and inserted a foam lid to dampen secondary flows. Six turbulence levels were used in random order with a 10-min warm-up period at the beginning of each treatment; this interval was sufficient for the turbulence to become stationary. The grids were turned off for at least 2 h between treatments. The PIV image plane (22 cm high × 22 cm wide) was centered on the midsection between the two grids and provided a map of u and w, the velocity vectors in the x and z dimensions, respectively (Fig. 1). The ADV was mounted with the probe projecting through the side wall and the approximately 1-cm^3, cylindrical measurement volume located in the center of the tank. The measurement volume's longitudinal axis intersected and was perpendicular to the PIV plane. The ADV provided point measurements of u, w, and v, the velocity in the y dimension. The ADV recorded for 10 min at 10 Hz, while the PIV collected data for 5 min at 1 Hz (i.e., one image pair per second) and for 1.8 min at 7 Hz. We later repeated the sequence of turbulence levels and recorded ADV data for 10 min at 25 Hz. Both instruments were used to estimate dissipation rates.

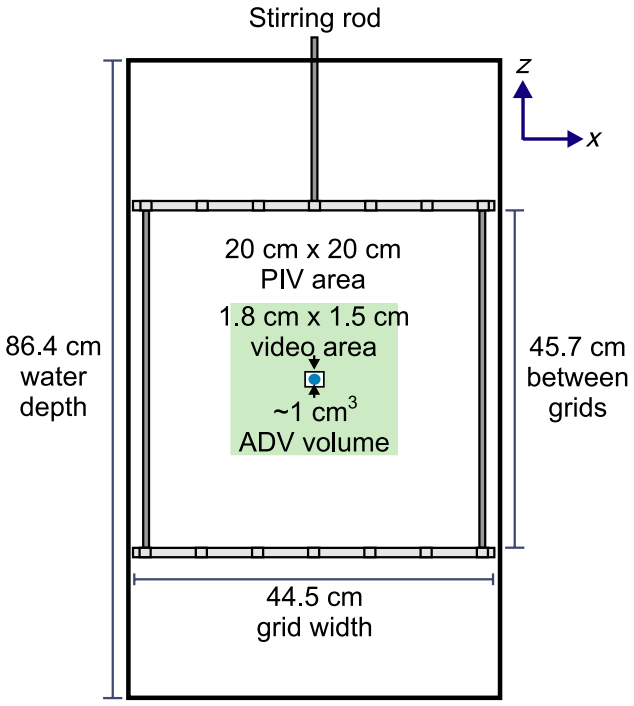

Fig. 1 Schematic of turbulence tank and measurement regions, approximately to scale. Large green square indicates area of PIV flow measurements; small white rectangle indicates area of larval video observations; small blue circle indicates area of ADV measurement volume. Coordinates x and z are noted in upper right, and y is the out-of-plane dimension.

[9] We estimated dissipation rates from PIV data as follows. PIV image pairs were processed using DaVis (LaVision) adaptive correlation algorithms to calculate velocity vectors u and w over nonoverlapping, 32×32 pixel interrogation windows ($\Delta x = 0.35$ cm resolution). The dissipation rate is defined as $\varepsilon = 2\nu\overline{s_{ij}s_{ij}}$, where the overbar denotes ensemble averaging, $s_{ij} = 0.5(\partial u_i/\partial x_j + \partial u_j/\partial x_i)$ is strain rate, and $i, j = 1, 2, 3$ are indices of spatial dimension. For planar measurements, ε can be simplified using the continuity equation and the fact that out-of-plane velocity gradients have similar magnitudes as in-plane gradients (e.g., Fincham et al. 1996). Rather than assuming isotropy, we estimated ε_P, the dissipation rate from PIV, directly from all measured velocity gradients as

$$\varepsilon_P(x,z) = 3\nu\left[\overline{\left(\frac{\partial u}{\partial x}\right)^2} + \overline{\left(\frac{\partial w}{\partial z}\right)^2} + \overline{\left(\frac{\partial u}{\partial z}\right)^2} + \overline{\left(\frac{\partial w}{\partial x}\right)^2} + 2\overline{\left(\frac{\partial u}{\partial z}\frac{\partial w}{\partial x}\right)} + \frac{2}{3}\overline{\left(\frac{\partial u}{\partial x}\frac{\partial w}{\partial z}\right)}\right] \quad (1)$$

(Doron et al. 2001). We also calculated ε_{P_c} as an average of ε_P over the center 1 cm^2 of the plane to estimate the dissipation rate at the location of ADV measurements.

[10] We estimated dissipation rates from the ADV data as follows. The ADV provides a time series of u, v, and w at a single point. Typically the vertical root-mean-square (RMS) velocity w_{RMS} is used as a characteristic velocity scale to estimate the dissipation rate, but because of probe geometry, w_{RMS} was noise dominated at low turbulence levels. Instead we used the low-noise velocity component v_{RMS} and estimated the dissipation rate from ADV as $\varepsilon_A = v_{\mathrm{RMS}}^3/\ell$, where v_{RMS} is the RMS velocity perpendicular to the PIV plane, $\ell = 0.2z$ is a length scale, and z is distance from the grids (Tennekes and Lumley 1972; McKenna 2000). These estimated ε_A gave a reasonable match to the PIV estimates ε_{P_c} and were further corrected as described below.

[11] During larval experiments only the ADV could be used for flow measurements because green PIV lasers affect the behavior of light-sensitive plankton (e.g., Yen et al. 2008). ADV estimates of dissipation rate were expected to be less accurate than PIV estimates because the ADV velocity vectors were calculated over a larger volume of water. When ε_A and ε_{P_c} were measured simultaneously, ε_A typically underestimated the dissipation rates, with larger discrepancies in weaker turbulence. To improve the ADV estimates, we calibrated them using the simultaneous PIV and ADV measurements. We related the PIV estimates and ADV estimates using a linear regression on a $\log_{10} - \log_{10}$ scale:

$$\log_{10}\varepsilon_{P_c} = a_0 + a_1\log_{10}\varepsilon_A. \quad (2)$$

Regressions were done separately for 10-Hz and 25-Hz ADV data. Lastly, we corrected dissipation estimates from the larval experiments as $\log_{10}\varepsilon_{A'} = \hat{a}_0 + \hat{a}_1\log_{10}\varepsilon_A$, where $\hat{a}_0$ and $\hat{a}_1$ are parameters estimated from equation (2) for 10-Hz data (Fig. 2).

Behavior Experiments

[12] Our experiments were designed to test whether mussel larval responses to turbulence vary with age or light conditions. To determine if responses to turbulence

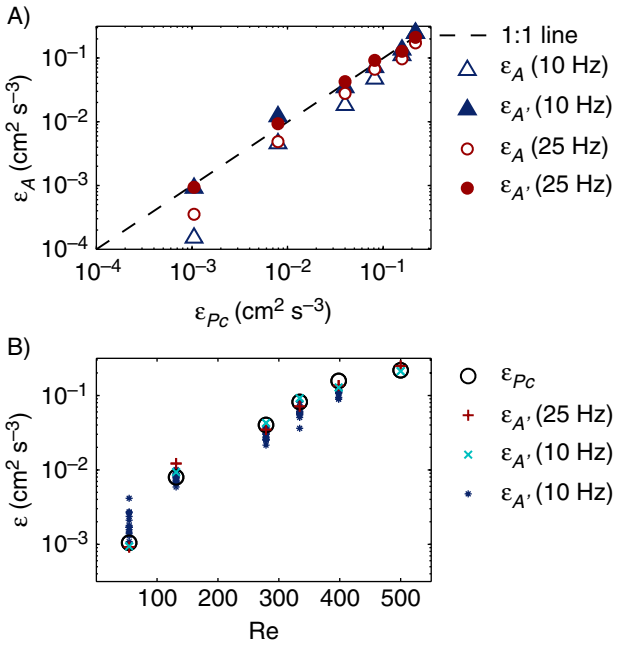

Fig. 2 Summary of dissipation rates in turbulence treatments. (A) Dissipation rates ε_A from ADV versus ε_{P_c} from PIV. ADV estimates are shown for 10-Hz (triangles) and 25-Hz (circles) data, including direct (open symbols) and adjusted (equation (2); closed symbols) estimates. (B) Dissipation rates versus Reynolds number. Separate ε estimates are from PIV data in center 1 cm^2 (circles), ADV 25-Hz data (x; adjusted), ADV 10-Hz data collected during PIV measurements (+; adjusted), and ADV 10-Hz data collected during larval experiments (*; adjusted).

changed ontogenetically, we repeated all experiments with young and old larvae. To determine if the response to turbulence was altered by lighting conditions, we repeated each set of turbulence treatments in light and dark. Dark conditions were maintained by installing black foam board over the tank walls and floor, with circular openings for the video camera and infrared spotlight used for video illumination. A black felt curtain was installed over the camera and light to minimize light leakage from the sides, and a foam insert prevented light from entering at the surface. For light conditions, the black coverings were removed and the tank was exposed to ambient overhead room lighting. We did not measure light intensity, but the room light was relatively weak and probably was representative of daytime in the subsurface ocean.

[13] The experiments closely followed the design used by Fuchs et al. (2004), with larvae exposed to alternating periods of still water and turbulence. Different larvae were used for each replicate in either light or dark conditions. At the beginning of each replicate we gently added larvae (0.1–0.4 larvae mL^{-1}) and food algae (*I. galbana*; $2–4 \times 10^3$ cells mL^{-1}) to the tank. The food algae were used as seeding particles for the ADV because artificial particles disrupt the behavior of bivalve larvae (H. L. Fuchs, unpubl.). After an initial 15-min acclimation period, we recorded larval movements in still water for 15 min using video. We then applied five turbulence treatment levels in a randomized sequence determined by a Latin square, with still-water rest periods of at least 10 min between treatments. Each turbulence treatment included an initial 10-min spin-up period followed by a period of video recording. The recording time and frame rate varied with the treatment level (4–15 min and 5–15 Hz, respectively) to account for the increased observation rate and frame-to-frame travel distance at higher water velocities. Experiments in both light and dark were replicated five times for young larvae, but we discarded the first two light replicates because dust and fibers had accumulated in the tank and interfered with video analysis. For old larvae only three replicates could be completed before all larvae had settled.

[14] We recorded the movements of mussel larvae in still water and turbulence using digital video. The video region was 1.8 cm × 2.5 cm, centered midway between the stirring grids (Fig. 1), and was illuminated by an infrared (810 nm) spotlight. Larval motions were recorded with an infrared-sensitive video camera (model KPF-120; Hitachi, Japan) and image capture software (EPIX XCAP; EPIX, Inc., USA). The ADV measured water velocity continuously at 10 Hz in the center of the video region, and the measurement volume overlapped with about a quarter of the video area. The velocity measurements enabled us to correct larval velocities for advection and to estimate turbulence dissipation rates during larval experiments.

Behavior Analysis

[15] Only the vertical velocity component is much affected by behavior or influences larval vertical fluxes (e.g., Eckman et al. 1994; Hansen et al. 1997), so analyses were based on larval vertical velocities w_L. Larval trajectories were reconstructed using a custom particle-tracking algorithm in Matlab (Fuchs et al. 2004). The number of trajectories ranged from 486 to 2867 per treatment, where a treatment is defined by turbulence level, larval age, and light conditions. Tracks had mean and maximum lengths of 1.1 ± 0.6 cm and 5.5 cm and mean and maximum durations of 2 ± 3.2 s and 60 s, respectively. Within a trajectory, the larval velocities are statistically dependent and autocorrelated, so we used a single vertical velocity measurement from each trajectory at the point where larvae were nearest the center of the video frame. Averaging these representative velocities provides a pseudo-Eulerian estimate of the mean observed larval velocity for each treatment. In turbulence the observed larval velocities include contributions from both behavior and flow. These separate motions are additive because larvae have a low particle Reynolds number ($Re = w_L d/\nu$, where d is the size of the larva; $\lesssim 1$) and negligible inertia (e.g., Reeks 1977). We corrected for advection by subtracting the mean water velocity (measured by ADV) from the mean observed larval velocity to get a spatially and temporally averaged behavioral velocity $\langle w_L \rangle$ at each treatment/replicate.

[16] Mixture models have been used to estimate the fraction of mud snail larvae that were swimming, hovering, and sinking (Fuchs et al. 2004). These behavior modes are typical of veligers (e.g., Gallager 1993;

Hansen et al. 1997) and were distinguishable by their characteristic velocity distributions with distinct peaks. For mussel larvae the mean velocities of swimmers and hoverers differed by $< 2\ \mathrm{mm\ s^{-1}}$ in still water, and these peaks became indistinct in turbulence as the variances were dominated by water velocity. The mixture model algorithm has low power to distinguish groups with similar means and large variances, so we used that approach only for larvae in still water.

[17] Behavioral mixtures were analyzed for still-water data pooled over each treatment: young + light, young + dark, old + light, and old + dark. We fitted a normal mixture model to w_L using an expectation-maximization algorithm to maximize the log-likelihood of the data (McLachlan and Peel 2000). For each behavior mode i we estimated the fraction α_i of larvae behaving in that mode and the mean μ_i and variance σ_i^2 of vertical velocities (for method details, see DiBacco et al. 2011). Although three behavior modes have been observed in veligers, we could not assume a priori that mussel veligers always had exactly three modes. We fitted the model for one to four behavior modes and used a Bayesian information criterion (e.g., Zucchini 2000) to determine the number of modes. Small larvae had two modes and large larvae had three modes.

[18] For larvae in turbulence, we focused on how the larval vertical velocity varied with dissipation rate. The average larval vertical velocity $\langle w_L \rangle$ varied nonlinearly with the dissipation rate $\varepsilon_{A'}$, so we modeled $\langle w_L \rangle$ as a function of $\varepsilon_{A'}$ using a logistic-type model,

$$\langle w_L \rangle = b_0 + \frac{b_1}{1 + \exp(-b_2 - b_3 \log_{10} \varepsilon_{A'})}, \qquad (3)$$

where b_0 and $b_0 + b_1$ are upper and lower bounds on larval velocity and the fraction $1/(1 + \exp(-b_2 - b_3 \log_{10}\varepsilon_{A'}))$ varies from 0 to 1. This model accounts for both the physical limits on swimming and sinking velocities and the potential switch in behaviors at a threshold level. We fitted the model to our experimental data using nonlinear regression to estimate the parameters $\hat{\phi} = [\hat{b}_0, \hat{b}_1, \hat{b}_2, \hat{b}_3]$.

Hypothesis Testing

[19] A fundamental question is whether larval age, light conditions, or turbulence affect the mean larval vertical velocity. We addressed this question using a three-factor analysis of variance (ANOVA) on all representative vertical velocities. When the ANOVA detected significant interaction among the three factors, we used a two-factor ANOVA for each turbulence level to determine if age and lighting effects were persistent.

[20] Using the fitted behavior model (equation (3)), we tested several nested hypotheses about the larval response to turbulence:

H_1: Young larvae behave differently in light and dark.

H_2: Old larvae behave differently in light and dark.

H_3: Young and old larvae behave differently in light.

H_4: Young and old larvae behave differently in dark.

H_5: Larvae behave differently in light and dark.

H_6: Young and old larvae behave differently.

The null hypothesis was that behavior did not differ among groups or treatments. We evaluated these hypotheses using a likelihood ratio (LR) test. The LR statistic for testing a null hypothesis H_0 against an alternative hypothesis H_x is

$$\Lambda = 2\left[\log L(\hat{\phi}_x) - \log L(\hat{\phi}_0)\right], \qquad (4)$$

where L is the likelihood and $\hat{\phi}_0$ and $\hat{\phi}_x$ are the parameter estimates under H_0 and H_x. In nonlinear regression the likelihood can be estimated as

$$L = \left(\frac{1}{\sqrt{2\pi\hat{\sigma}^2}}\right)^n \exp\left[-\frac{\sum_{i=0}^{n}\left[\langle w_L \rangle_i - f(\varepsilon_i, \hat{\phi})\right]^2}{2\hat{\sigma}^2}\right], \qquad (5)$$

Table 1 Summary of flow statistics from PIV averaged over the middle 1 $\mathrm{cm^2}$ of video region. Level indicates turbulence tank setting, f is the stirring frequency, Re is the Reynolds number, w_{RMS}/u_{RMS} is the isotropy ratio, ε is the dissipation rate, η is the Kolmogorov length scale, and λ is the Taylor microscale.

Level	f(Hz)	Re	w_{RMS}/u_{RMS}	ε ($\mathrm{cm^2\ s^{-3}}$)	η (cm)	λ (cm)
1	0.14	54	0.96	1.0×10^{-3}	0.18	1.36
2	0.41	131	1.01	7.9×10^{-3}	0.11	1.27
3	0.67	279	1.00	4.0×10^{-2}	0.07	1.18
4	0.94	334	1.30	8.1×10^{-2}	0.06	1.28
5	1.20	398	1.24	1.6×10^{-1}	0.05	1.06
6	1.45	500	1.25	2.2×10^{-1}	0.05	1.13

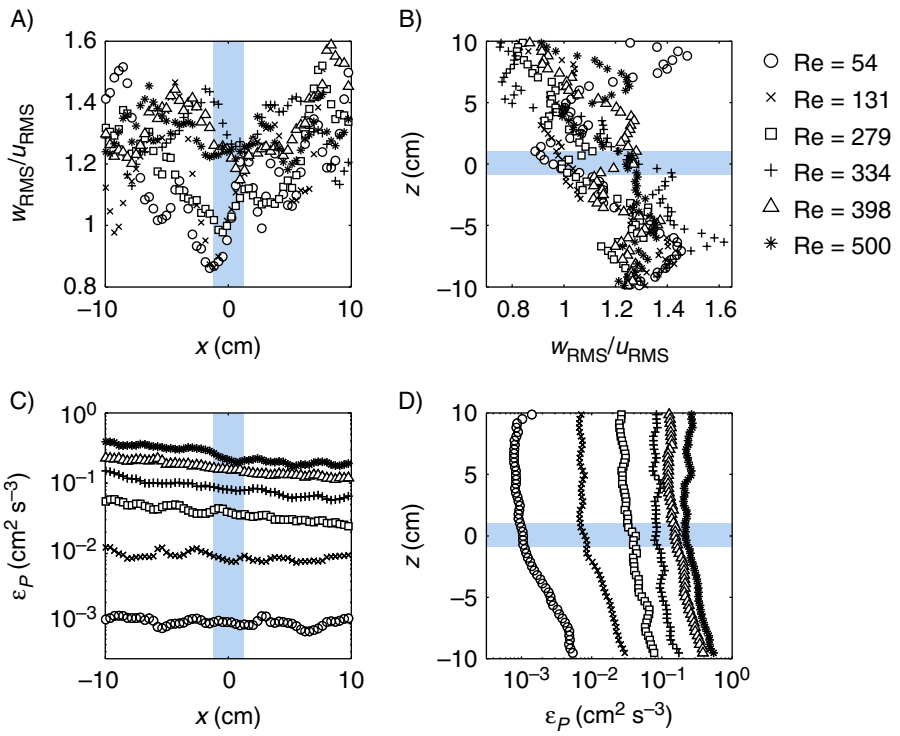

Fig. 3 Summary of flow statistics from PIV versus distance from center of tank: (A) w_{RMS}/u_{RMS} versus horizontal distance x, (B) w_{RMS}/u_{RMS} versus vertical distance z, (C) ε_P versus horizontal distance x, and (D) ε_P versus vertical distance z. Shaded blue rectangles indicate overlap with larval observation region.

where $\hat{\sigma}^2$ is the variance of the residuals, n is the number of observations, $\langle w_L \rangle_i$ is the observed mean larval velocity for $i = 1$ to n, and $f(\varepsilon_i, \hat{\phi})$ is the modeled larval velocity given the parameter estimates $\hat{\phi}$ (McCullagh and Nelder 1989). This likelihood function assumes that the residuals are normally distributed, so we used a Lilliefors test to confirm that a normal distribution could not be rejected for any group of residuals. The test statistic Λ is χ^2 distributed, with degrees of freedom equal to the number of parameters under H_x minus the number of parameters under H_0. We rejected the null hypothesis when $\Lambda > \chi^2$ with 4 degrees of freedom and a significance level of $\alpha = 0.05$.

Results

Turbulence

[21] The grid oscillation frequency ranged from 0.14 to 1.45 Hz for the six turbulence treatments used (Table 1). These treatments had Reynolds numbers ($\mathrm{Re} = u_{\mathrm{RMS}}\ell/\nu$, where u_{RMS} is calculated from PIV data) of 54–500 and produced dissipation rates of 1.0×10^{-3} to 2.2×10^{-1} cm^2 s^{-3} (Fig. 2). Dissipation rates from the PIV generally differed from uncorrected ADV estimates by less than a factor of 2, and the correction in equation (2) reduced this difference to less than a factor of 1.2. A larger correction was needed for the 10-Hz ADV data ($\hat{a}_0 = 0.76$ and $\hat{a}_1 = -0.22$) than for the 25-Hz data ($\hat{a}_0 = 0.87$ and $\hat{a}_1 = -0.09$), which captured more of the high-frequency velocity fluctuations. The Taylor microscale ($\lambda = (15\nu w_{\mathrm{RMS}}^2/\varepsilon)^{0.5}$), which is a measure of the average eddy length scale, ranged from 1.05 to 1.36 cm.

[22] Turbulence was most nearly isotropic at lower stirring frequencies and near the center of the tank where the video observations were made (Fig. 3). The isotropy ratio $w_{\mathrm{RMS}}/u_{\mathrm{RMS}}$ varied from approximately 0.8 to 1.6 but was generally closest to 1.0 at the midpoint and remained fairly steady within the approximately 5 cm above the midpoint (Fig. 3A, B). Isotropy ratios were slightly more variable than those in tanks with turbulence generated by a single grid (Hopfinger and Toly 1976; De Silva and Fernando 1994) or jet actuators (Hwang and Eaton 2004; Webster et al. 2004) but no greater than those in other double-grid tanks (Srdic et al. 1996; Shy et al. 1997). Some anisotropy can be attributed to unavoidable secondary circulations (e.g., McKenna and McGillis 2004). Dissipation rates were estimated without assuming isotropy and were relatively homogeneous both horizontally and vertically (Fig. 3C, D). Normalized dissipation rates ($\varepsilon_P/\varepsilon_{P_0}$, where ε_{P_0} is a spatial average) were generally between 0.7 and 1.3 over a 10 cm × 10 cm area, comparing favorably with the homogeneity of dissipation in jet tanks (Webster et al. 2004). The relative homogeneity of ε_P

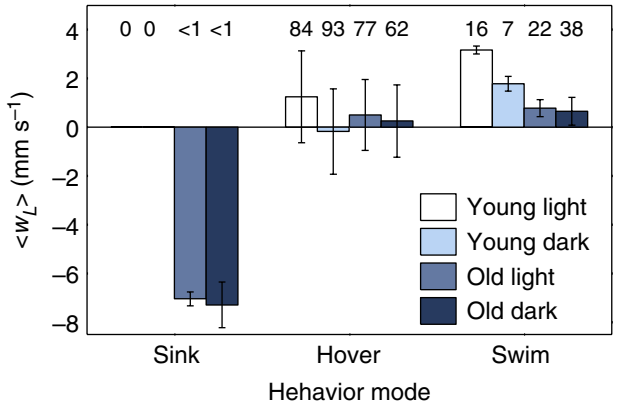

Fig. 4 Three behavior modes exhibited by larvae in still water, shown as mean velocity ± 1 SD for larvae in each mode. Numbers above each bar indicate the percentage of larvae in a given treatment behaving in that mode. Bar colors indicate treatment (white, young larvae in light; light blue, young larvae in dark; medium blue, old larvae in light; dark blue, old larvae in dark).

ensures that $\varepsilon_{A'}$ measured during the larval experiments is representative of dissipation rates larvae would have encountered in a large area outside where larvae were observed.

[23] PIV can fail to capture the smallest-scale motions at higher turbulence levels as the interrogation window Δx becomes relatively larger compared to the Kolmogorov scale η. Dissipation rates calculated by the direct method (equation (1)) are highly accurate when $\Delta x/\eta < 3$ but can be underestimated at larger values of $\Delta x/\eta$ (e.g., Antonia et al. 1994; Tanaka and Eaton 2007; de Jong et al. 2009). Alternatively, the vector resolution should be less than 30% of the Taylor microscale λ (Saarenrinne and Piirto 2000). Here $\Delta x/\eta$ ranged from 1.9 to 7.3 (6.7 for larval treatments), and Δx was 26%–33% of λ. Based on the $\Delta x/\eta$ criterion, ε may have been underestimated by approximately 20% at the highest turbulence levels (Antonia et al. 1994). An underestimate of 20% would mean that the dissipation rate at Re = 500, for example, was really $\varepsilon = 2.6 \times 10^{-1}\,\mathrm{cm^2\,s^{-3}}$ rather than the estimated $2.2 \times 10^{-1}\,\mathrm{cm^2\,s^{-3}}$. These potential errors in dissipation rate are small on the $\log_{10}$ scale over which $\langle w_L \rangle$ varies, and we made no attempt to correct them.

Larval Behavior

[24] In still water, larvae exhibited three behavior modes (Fig. 4) similar to the sinking, hovering, and swimming modes observed previously in veliger larvae. Passive sinking was observed only in old larvae and accounted for <1% of observations, with mean sinking velocities of −7.0 and $-7.3\,\mathrm{mm\,s^{-1}}$ in light and dark, respectively. All groups had a second behavior mode with a mean velocity magnitude of $<1.25\,\mathrm{mm\ s^{-1}}$ and relatively large standard deviation ($>1.4\,\mathrm{mm\ s^{-1}}$), indicating that larvae were swimming both up and down. This behavior probably corresponded to the hovering mode, although hovering velocities typically have a near-zero mean and small variance (Gallager 1993; Fuchs et al. 2004). The third behavior mode had a strictly positive mean velocity ($0.65–3.2\,\mathrm{mm\ s^{-1}}$) and small standard deviation ($<0.6\,\mathrm{mm\ s^{-1}}$) and corresponded to upward swimming. Mean velocities of the hovering and swimming modes were slightly higher for young larvae than for old larvae and higher in light conditions than in dark conditions.

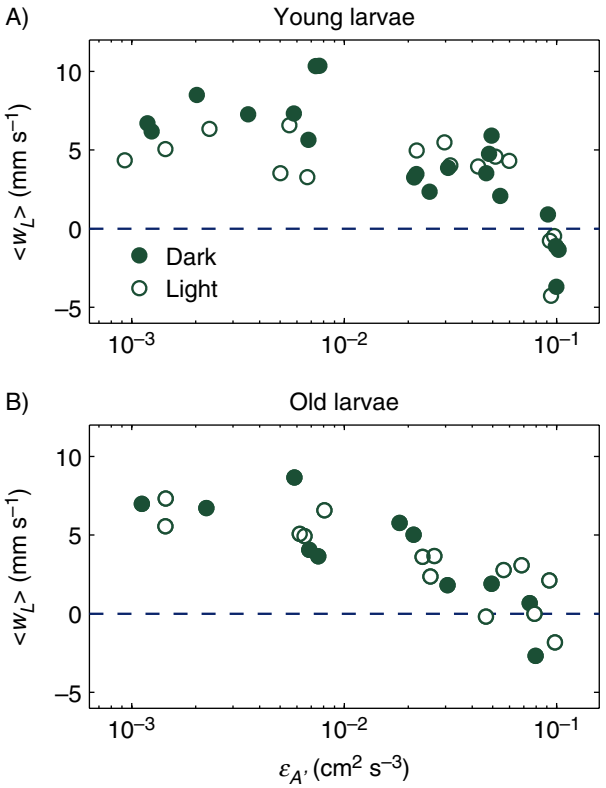

Fig. 5 Larval vertical velocity $\langle w_L \rangle$ versus dissipation rate $\varepsilon_{A'}$ for (A) veliconcha larvae and (B) eyed veligers in light (open circles) and dark (closed circles) conditions. Data are averaged over individual treatment replicates, and dashed line indicates neutral buoyancy.

Table 2 Results of three-factor ANOVA on mean larval velocity $\langle w_L \rangle$, with degrees of freedom *df*, mean squares *MS*, *F* statistic, and *p*-value. Significance level $\alpha = 0.05$.

Source	*df*	*MS*	*F*	*p*
Age	1	447	8.05	0.005
Lighting	1	6213	111.87	< 0.001
Turbulence	5	35 184	633.47	< 0.001
Age × lighting	1	940	16.92	< 0.001
Age × turbulence	5	7217	129.94	< 0.001
Light × turbulence	5	1582	28.48	< 0.001
Age × lighting × turbulence	5	3077	55.39	< 0.001
Error	35 644	55.5		

[25] The mean larval vertical velocity was more affected by turbulence than by either larval age or light conditions (Fig. 5). In weaker turbulence, larvae swam upward with mean vertical velocities of up to $\langle w_L \rangle = 10.8$ mm s^{-1}. In the strongest turbulence, however, larvae were generally sinking, with mean vertical velocities reaching $\langle w_L \rangle = -4.3$ mm s^{-1}. Mean larval velocities were significantly affected by all three factors and their interactions (Table 2), but the effects of larval age and light were sometimes not significant at higher turbulence levels (Table 3). Note that sample sizes were large, so ANOVA had high power and was sensitive to small differences in $\langle w_L \rangle$. For example, with a power of $\beta = 0.9$ and a significance level of $\alpha = 0.5$, there were enough observations to detect differences in $\langle w_L \rangle$ as small as 0.1–0.8 mm s^{-1}. Despite the ANOVA finding of significant differences, the modeled relationship between larval vertical velocity and dissipation rate was similar for young and old larvae under light and dark conditions. There were no statistical differences in parameters $\hat{\phi}$ of the behavior model (equation (3)) for any paired comparison (Table 4).

[26] Given that larvae responded similarly to turbulence regardless of age or lighting, we present the model fit for all data combined (Fig. 6). The fitted parameter estimates (equation (3); $\hat{b}_0 = 6.4$, $\hat{b}_1 = -697$, $\hat{b}_2 = -4.4$, $\hat{b}_3 = 2.4$) gave population-averaged vertical velocities that switched from positive (upward) in weaker turbulence to negative (downward) in stronger turbulence. The velocity shift occurred at a threshold (or critical) dissipation rate of $\varepsilon_{cr} = 8.3 \times 10^{-2}$ cm^2 s^{-3}, where the subscript cr refers to a critical value, corresponding to a Kolmogorov length scale of $\eta_{cr} = 0.059$ cm and a shear of $\gamma_{cr} = 0.74$ s^{-1}, where $\gamma = (\varepsilon_{A'}/15\nu)^{0.5}$. The modeled upper bound on larval velocity ($\hat{b}_0 = 6.4$ mm s^{-1}) was comparable to swimming velocities measured for larvae in still water. The functional form of $\langle w_L \rangle$ also has a lower bound ($\hat{b}_0 + \hat{b}_1$), but that value had no biological meaning here because larvae did not reach a maximum sinking speed within the tested range of dissipation rates. We expect that the true lower bound on velocity would approximate the passive sinking velocity (approx. -7 mm s^{-1}).

Discussion

[27] Mussel larvae sank at high dissipation rates ($\varepsilon_{cr} > 8.3 \times 10^{-2}$ cm^2 s^{-3}) that are common in coastal currents, and this behavior should enhance their flux to the bed in nearshore areas. Larvae may succeed by land-

Table 3 Results of two-factor ANOVA on mean larval velocity $\langle w_L \rangle$ evaluated at each turbulence level (indicated by Re), with degrees of freedom *df*, mean squares *MS*, *F* statistic, and *p*-value. Significance level $\alpha = 0.05$.

Re	Source	*df*	*MS*	*F*	*p*
0	Age	1	18.2	6.37	0.012
	Lighting	1	1086	380.29	< 0.001
	Age × lighting	1	118	41.13	< 0.001
	Error	4122	2.86		
54	Age	1	2620	116.37	< 0.001
	Lighting	1	7094	315.13	< 0.001
	Age × lighting	1	3260	144.8	< 0.001
	Error	2224	22.5		
131	Age	1	10 346	227.04	< 0.001
	Lighting	1	715	15.69	< 0.001
	Age × lighting	1	1402	30.77	< 0.001
	Error	4689	45.6		
279	Age	1	73.4	1.05	0.306
	Lighting	1	259	3.70	0.054
	Age × lighting	1	7474	106.87	< 0.001
	Error	8240	70.0		
334	Age	1	22 392	348.33	< 0.001
	Lighting	1	611	9.50	0.002
	Age × lighting	1	1174	18.27	< 0.001
	Error	10 237	64.3		
398	Age	1	7480	96.57	< 0.001
	Lighting	1	1.10	0.01	0.907
	Age × lighting	1	359	4.63	0.031
	Error	6961	77.5		

Table 4 LR test statistics and *p*-values for hypothesis tests about fitted parameters for modeled larval response to turbulence (equation (3)). Subscripts on $\hat{\phi}$ indicate the group used to estimate parameters. Significance level $\alpha = 0.05$, and degrees of freedom $df = 4$.

Alternative hypothesis	Λ	*p*
H_1: $\hat{\phi}_{\text{young,light}} \neq \hat{\phi}_{\text{young,dark}}$	8.39	0.08
H_2: $\hat{\phi}_{\text{old,light}} \neq \hat{\phi}_{\text{old,dark}}$	3.33	0.50
H_3: $\hat{\phi}_{\text{young,light}} \neq \hat{\phi}_{\text{old,light}}$	7.83	0.10
H_4: $\hat{\phi}_{\text{young,dark}} \neq \hat{\phi}_{\text{old,dark}}$	4.38	0.36
H_5: $\hat{\phi}_{\text{light}} \neq \hat{\phi}_{\text{dark}}$	7.53	0.11
H_6: $\hat{\phi}_{\text{young}} \neq \hat{\phi}_{\text{old}}$	8.02	0.09

ing near a suitable habitat, because although *Mytilus* spp. tend to settle first on filamentous substrates (Eyster and Pechenik 1988; Cáceres-Martínez et al. 1994), they are commonly transported as postlarvae to other locations (Cáceres-Martínez et al. 1994; Hunt and Scheibling 1998). Young mussels are often dislodged from their initial settlement sites by storms or ice scour and then use mucus or byssus threads to drift to secondary settlement sites (Lane et al. 1985; Cáceres-Martínez et al. 1994; Hunt and Scheibling 1998). Because postlarvae are bigger and more negatively buoyant than swimming veligers, they should remain closer to the bottom and may be more successful at locating patchily distributed adult mussels. For larvae, however, turbulence-induced sinking would increase the probability of contacting primary settlement sites in energetic coastal waters (e.g., Fuchs et al. 2007).

[28] Larvae that sink in strong turbulence would be more likely to land on a rough substrate than on a smooth one, which should also raise the probability of settling on mussel beds. Rough, hard substrates generally have higher drag coefficients than sandy sediments. For example, drag coefficients at 1 m above bottom over horse mussel beds (*Atrina zelandica*) are $C_d = 0.008$ to 0.01, a factor of 3–4 higher than C_d over flat sand (Green et al. 1998). Given that drag and the free-stream velocity U determine shear velocity as $u_* = C_d^{0.5} U$ (the quadratic drag law) and dissipation rate is $\varepsilon \approx u_*^3/\kappa z$, where $\kappa = 0.41$ is von Kármán's constant, then at a given U the ε would be five to eight times higher over mussel beds than over sand. The resulting larval velocities could be more negative by several millimeters per second, giving larvae a greater sinking flux over mussel beds than over fine sediments.

[29] Contrary to our expectations, mussel larvae began sinking at a threshold dissipation rate no higher than the thresholds for gastropod larvae. At this threshold the Kolmogorov length scale is $\eta_{cr} = 590$ μm, two to three times the larval length including the velum. Over distances smaller than η, shear is laminar (Lazier and Mann 1989), and a η_{cr} larger than the larvae

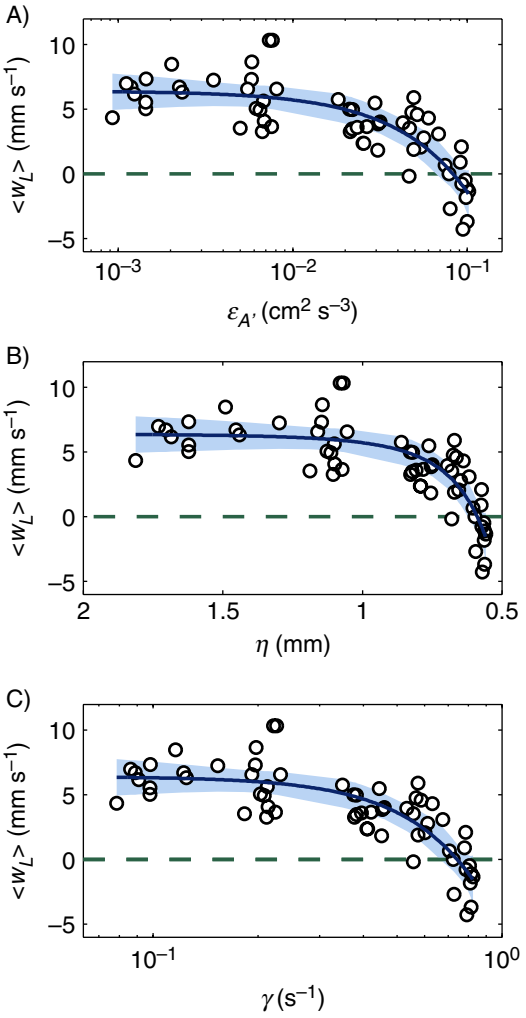

Fig. 6 Larval vertical velocity $\langle w_L \rangle$ versus (A) dissipation rate $\varepsilon_{A'}$, (B) Kolmogorov length scale η, and (C) shear γ. The η axis is reversed because small η corresponds to large ε. Symbols are data averaged over individual treatment replicates; dashed line indicates neutral buoyancy; solid line is equation (3) fitted by nonlinear regression; shaded area indicates a 95% prediction interval. Average larval velocity switches from positive to negative at $\varepsilon_{cr} = 8.3 \times 10^{-2}$ cm^2 s^{-3}, $\eta_{cr} = 0.59$ mm, and $\gamma_{cr} = 0.74$ s^{-1}.

implies that larvae sense turbulence by its magnitude rather than by its length scale. The turbulence detection mechanism apparently is independent of the length of the velum but may instead depend on detection limits for mechanical stimulation of cilia. Touch elicits ciliary arrest in snail veligers and in cilia from gills of adult *M. edulis* (Murakami and Takahashi 1975; Mackie et al. 1976), but measurements of the threshold for mechanoreception are lacking. Alternatively, shear may enable larvae to detect turbulence using the statocysts if the viscous torque across the body exceeds the gravitational torque, rotating the larvae away from their normal velum-up orientation (e.g., Jonsson et al. 1991). Here the threshold mean shear for sinking was $\gamma_{cr} = 0.7\ s^{-1}$, compared to $\gamma_{cr} = 1.6\ s^{-1}$ and $\gamma_{cr} = 0.4–0.8\ s^{-1}$ for snail larvae in previous studies (Fuchs et al. 2004, 2010). These threshold shears are all within an order of magnitude of one another, but it is unclear whether they are constrained by larval physiology or by adaptation to similar flow regimes.

[30] Mussel larvae also had noticeably higher velocities in weak turbulence than in still water, probably because flow conditions influence which behavior mode optimizes the trade-off between larval feeding and signaling to potential predators. In still water most larvae (62%–93%) were hovering and the overall mean velocities were near zero, whereas in weak turbulence the mean velocities were in the range measured for swimming larvae (approx. 6 to 7 mm s^{-1}). A similar switch was observed in mud snail larvae that mainly hovered (approx. 0 mm s^{-1}) in still water but mainly swam upward (approx. 3 to 4 mm s^{-1}) in weak turbulence (Fuchs et al. 2004). The switch from hovering to swimming may reflect a response to the apparent food availability. At a fixed algal concentration, larvae would encounter algae more frequently in turbulence than in still water (e.g., Rothschild and Osborn 1988). When food is sparse or patchy, hovering is a more effective feeding mode than swimming because it enables larvae to draw in more food particles from the side (Gallager 1988). Hovering is riskier than swimming, however, because it generates a larger hydrodynamic disturbance that is detectable to predators (Gallager 1988). The observed behavioral shift would enable larvae to maximize feeding in still water when food is encountered rarely and to minimize detection by predators in turbulence when food is encountered more often.

Methodological Considerations

[31] We used two different statistical approaches to test whether larval vertical velocity is affected by age, light, and turbulence, and the results highlight the difference between statistical and biological significance. The ANOVA finds significant effects of both age and light at most turbulence levels (Table 3), whereas the LR test finds no differences in larval responses to turbulence among age and light treatments (Table 4). This apparent contradiction arises because the statistics test different hypotheses. The ANOVA tests whether the mean velocity at a given treatment is significantly affected by the three factors. Each mean velocity is estimated from hundreds to thousands of trajectories, however, and the test is extremely sensitive to small differences (approx. 0.1 mm s^{-1}) in larval velocity. The LR provides a more relevant assessment of behaviors, testing for differences in the parameters of the fitted behavior model (larval velocity as a function of dissipation rate) among age and light treatments. The response to turbulence dominates the variation in larval vertical velocity, and Fig. 5 indicates that the effects of age or light on this response are negligible.

[32] The range of turbulence used in the mussel experiments was too limited to characterize the transition from hovering to swimming or to determine the maximum attainable sinking speeds. Turbulence levels were limited partly by the brevity of our visits to Woods Hole and partly because ε at the highest levels was lower during the larval studies than during the initial flow characterizations. These differences in dissipation rates may have arisen from working in two different buildings. The tank was moved and reassembled in a temperature-controlled room for the larval work, and changes in the electrical supply or tank assembly could have altered the relationship between tank settings and stirring frequency. In retrospect, we could have included more turbulence treatments by omitting the light or dark treatment. Despite the limited experimental design, our treatment choices enabled us to gain valuable empirical evidence that the larval response to turbulence is unaltered by larval age or lighting conditions.

Implications of Behavior for Vertical Distributions

[33] This multifactor behavior experiment provides some insights into apparently inconsistent evidence from previous studies. In earlier experiments with *M. edulis*, larval responses to light changed several times through development: D-stage larvae were negatively phototactic, veliconcha larvae had no response to light, and eyed veligers were positively phototactic (Bayne 1964b). These behaviors should cause larvae to be concentrated higher in the water column as they age, but field researchers report similar vertical distributions for mussel larvae of all sizes (Knights et al. 2006). The similar larval distributions may reflect some homogenization due to turbulent mixing, yet our results suggest that ontogeny and phototaxis would have little effect on vertical distributions. Here the mean larval velocity $\langle w_L \rangle$ varied by only $< 2\,\text{mm s}^{-1}$ in response to larval age or light, while $\langle w_L \rangle$ varied by up to $15\,\text{mm s}^{-1}$ in response to turbulence. Although these controlled experiments tested only a subset of potential cues, turbulence apparently has a large impact on veliger behavior even in the field. Behaviors were estimated for three genera of snail larvae in a tidal inlet where all potential cues varied, and responses to turbulence accounted for an estimated 46%–64% of the net behavior of competent larvae (Fuchs et al. 2010). Likewise for mussel larvae, the overall behavior and its effects on larval vertical distributions may be dominated by the response to turbulence.

[34] In the field, mussel larvae do have uneven vertical distributions that suggest an influence of turbulence on larval vertical migrations. Although field studies report different vertical distributions of *M. edulis* larvae, the data were collected in disparate flow regimes. In weaker currents (approx. $11\,\text{cm s}^{-1}$) larvae were most concentrated near the surface (Dobretsov and Miron 2001), whereas in strong currents (approx. 85 to $100\,\text{cm s}^{-1}$) larvae were most concentrated near the bottom (Knights et al. 2006). In a third study with both stratified and well-mixed sites, larvae were most concentrated at mid-depths, but the depth of maximum larval concentration was 2 m deeper during strong winds (Raby et al. 1994). These distributions provide only limited insights into behavior because they are also influenced by turbulent mixing and horizontal advection. The observations do imply that stronger currents and winds are associated with larvae concentrated lower in the water column, consistent with our findings that strong turbulence induces larvae to sink.

Potential Effects of Behavior on Dispersal

[35] Early-stage *M. edulis* larvae responded to turbulence, suggesting that the behavior occurs throughout development and would affect dispersal over large spatial scales (tens to hundreds of kilometers). Such larvae could sink in energetic flows to aid nearshore retention and minimize larval loss to the deeper ocean. Sinking would be effective for reducing dispersal when bottom currents are slower or more shoreward than surface currents. For example, in simulations of larval dispersal in Chesapeake Bay, the oysters *Crassostrea virginica* and *Crassostrea ariakensis* were modeled to swim up and down, respectively, upon encountering haloclines (North et al. 2008). *C. ariakensis* larvae spent comparatively more time in deeper waters that generally moved up-estuary, resulting in lower dispersal distances and higher self-recruitment. Similarly, mussel larvae could limit their dispersal in estuaries by sinking in strong turbulence associated with peak tidal currents. Sinking in turbulent coastal waters may also enable larvae to be retained near shore by asymmetric tidal mixing, which would tend to transport larvae up-slope and reduce loss of larvae to offshore waters (Pringle and Franks 2001). Genetic data suggest that *M. edulis* do disperse somewhat less than would be expected based on hydrodynamics alone, with some *M. edulis* populations being largely self-seeded (Gilg and Hilbish 2003; Gilg et al. 2007). Although hydrodynamic barriers were proposed as a cause of self-recruitment (Gilg et al. 2007), turbulence-induced sinking is a potential behavioral mechanism for limiting dispersal and enhancing retention near coastal habitats.

Significance to Aquatic Environments

[36] Mollusk larvae can swim or sink vertically through the water column, and their behaviors affect vertical positioning, large-scale horizontal transport, and the supply of larvae to benthic populations (Eckman et al. 1994; Fuchs et al. 2007; North et al. 2008). Although larvae react during settlement to chemicals from the benthos (e.g., Turner et al. 1994; Hadfield and Koehl

2004), chemicals typically are diluted to undetectable levels within a few centimeters of the bed (e.g., Crimaldi and Koseff 2001; Koehl et al. 2007), and large-scale dispersal would be more affected by responses to cues in the water column. Larval responses to hydrodynamic cues such as velocity shear and turbulence (e.g., Pawlik and Butman 1993; Welch and Forward 2001) could aid dispersal into or away from specific flow regimes and may be adaptations for larval transport toward suitable adult habitats. This study quantified the responses of mussel larvae at two ages to two physical properties associated with shallow coastal habitats: light and turbulence. Larvae sank in turbulence above a threshold whose value indicates that veligers can detect turbulence despite being smaller than the smallest eddies. Results also show that the larval responses to light that were observed in still water have little impact on the overall behavior in turbulence, underscoring the importance of studying larval behaviors in biologically relevant flow conditions (e.g., Koehl and Reidenbach 2007). In energetic coastal waters, larvae that sink in turbulence could improve their odds of being retained near shallow habitats and settling onto adult mussel beds. This study provides a quantitative behavior model that can be used with large-scale numerical simulations of larval dispersal to test hypotheses about how responses to turbulence affect where larvae disperse and settle.

Acknowledgments We thank S. Feindel at the Darling Marine Center for providing the mussel larvae and food algae and K. Helfrich for providing PIV guidance and instrument loans. F. Thwaites designed the turbulence tank, L. Nasmith measured the larvae, L. Mullineaux assisted with flow measurements and tank assembly, and K. Douglas assisted with particle tracking. J. P. Grassle, J. Wilkin, J. Ackerman, and two anonymous reviewers provided helpful comments on the manuscript. This research was funded by the Woods Hole Oceanographic Institution Coastal Ocean Institute and the Woods Hole Sea Grant Program (National Oceanic and Atmospheric Administration grant NA06OAR4170021, project R/B-173).

References

Antonia, R. A., Y. Zhu, and J. Kim. 1994. Corrections for spatial velocity derivatives in a turbulent shear flow. Exp. Fluids. **16**: 411–413, doi:10.1007/BF00202066.

Barile, P. J., A. W. Stoner, and C. M. Young. 1994. Phototaxis and vertical migration of the queen conch (*Strombus gigas* Linne) veliger larvae. J. Exp. Mar. Biol. Ecol. **183**: 147–162, doi:10.1016/0022-0981(94)90084-1.

Bayne, B. L. 1964a. Primary and secondary settlement in *Mytilus edulis* L. (Mollusca). J. Anim. Ecol. **33**: 513–523, doi:10.2307/2569.

Bayne, B. L. 1964b. The responses of the larvae of *Mytilus edulis* L. to light and gravity. Oikos. **15**: 162–174, doi:10.2307/3564753.

Brumley, B. H., and G. H. Jirka. 1987. Near-surface turbulence in a grid-stirred tank. J. Fluid Mech. **183**: 235–263, doi:10.1017/S0022112087002623.

Cáceres-Martínez, J., J. A. F. Robledo, and A. Figueras. 1994. Settlement and post-larval behaviour of *Mytilus galloprovincialis*: Field and laboratory experiments. Mar. Ecol. Prog. Ser. **112**: 107–117, doi:10.3354/meps112107.

Crimaldi, J. P., and J. R. Koseff. 2001. High-resolution measurements of the spatial and temporal scalar structure of a turbulent plume. Exp. Fluids. **31**: 90–102, doi:10.1007/s003480000263.

de Jong, J., L. Cao, S. H. Woodward, J. P. L. C. Salazar, L. R. Collins, and H. Meng. 2009. Dissipation rate estimation from PIV in zero-mean isotropic turbulence. Exp. Fluids. **46**: 499–515, doi:10.1007/s00348-008-0576-3.

De Silva, I. P. D., and H. J. S. Fernando. 1994. Oscillating grids as a source of nearly isotropic turbulence. Phys. Fluids. **6**: 2455–2464, doi:10.1063/1.868193.

DiBacco, C., H. L. Fuchs, J. Pineda, and K. R. Helfrich. 2011. Swimming behavior and velocities of barnacle cyprids in a downwelling flume. Mar. Ecol. Prog. Ser. **433**: 131–148, doi:10.3354/meps09186.

Dillon, T. M., and D. R. Caldwell. 1980. The Batchelor spectrum and dissipation in the upper ocean. J. Geophys. Res. **85**: 1910–1916, doi:10.1029/JC085iC04p01910.

Dobretsov, S. V., and G. Miron. 2001. Larval and post-larval vertical distribution of the mussel *Mytilus edulis* in the White Sea. Mar. Ecol. Prog. Ser. **218**: 179–187, doi:10.3354/meps218179.

Doron, P., L. Bertuccioli, J. Katz, and T. R. Osborn. 2001. Turbulence characteristics and dissipation estimates in the coastal ocean bottom boundary layer from PIV data. J. Phys. Oceanogr. **31**: 2108–2134, doi:10.1175/1520-0485(2001)031<2108:TCADEI>2.0.CO;2.

Eckman, J. E., and D. O. Duggins. 1998. Larval settlement in turbulent pipe flows. J. Mar. Res. **56**: 1285–1312, doi:10.1357/002224098765093643.

Eckman, J. E., F. E. Werner, and T. F. Gross. 1994. Modelling some effects of behavior on larval settlement in a turbulent boundary layer. Deep Sea Res. Part II Top. Stud. Oceanogr. **41**: 185–208, doi:10.1016/0967-0645(94)90067-1.

Eyster, L. S., and J. A. Pechenik. 1988. Attachment of *Mytilus edulis* L. larvae on algal and byssal filaments is enhanced by water agitation. J. Exp. Mar. Biol. Ecol. **114**: 99–110, doi:10.1016/0022-0981(88)90131-1.

Fincham, A. M., T. Maxworthy, and G. R. Spedding. 1996. Energy dissipation and vortex structure in freely decaying, stratified grid turbulence. Dyn. Atmos. Oceans. **23**: 155–169, doi:10.1016/0377-0265(95)00415-7.

Finelli, C. M., and D. M. Wethey. 2003. Behavior of oyster (*Crassostrea virginica*) larvae in flume boundary layer flows. Mar. Biol. **143**: 703–711, doi:10.1007/s00227-003-1110-z.

Fuchs, H. L., L. S. Mullineaux, and A. R. Solow. 2004. Sinking behavior of gastropod larvae (*Ilyanassa obsoleta*) in turbulence. Limnol. Oceanogr. **49**: 1937–1948, doi:10.4319/lo.2004.49.6.1937.

Fuchs, H. L., M. G. Neubert, and L. S. Mullineaux. 2007. Effects of turbulence-mediated larval behavior on larval supply and settlement in tidal currents. Limnol. Oceanogr. **52**: 1156–1165, doi:10.4319/lo.2007.52.3.1156.

Fuchs, H. L., A. R. Solow, and L. S. Mullineaux. 2010. Larval responses to turbulence and temperature in a tidal inlet: Habitat selection by dispersing gastropods? J. Mar. Res. **68**: 153–188, doi:10.1357/002224010793079013.

Gallager, S. M. 1988. Visual observations of particle manipulation during feeding in larvae of a bivalve mollusc. Bull. Mar. Sci. **43**: 344–365.

Gallager, S. M. 1993. Hydrodynamic disturbances produced by small zooplankton: Case study for the veliger larva of a bivalve mollusc. J. Plankton Res. **15**: 1277–1296, doi:10.1093/plankt/15.11.1277.

Gilg, M. R., and T. J. Hilbish. 2003. The geography of marine larval dispersal: Coupling genetics with fine-scale physical oceanography. Ecology. **84**: 2989–2998, doi:10.1890/02-0498.

Gilg, M. R., S. E. Kirby, R. Sullivan, L. W. Knapp, and T. J. Hilbish. 2007. Dispersal vs. retention: Correspondence of species-specific reproductive cycles and settlement periods in a blue mussel hybrid zone. Mar. Ecol. Prog. Ser. **351**: 151–161, doi:10.3354/meps07145.

Green, M. O., J. E. Hewitt, and S. F. Thrush. 1998. Seabed drag coefficient over natural beds of horse mussels (*Atrina zelandica*). J. Mar. Res. **56**: 613–637, doi:10.1357/002224098765213603.

Gross, T. F., and A. R. M. Nowell. 1985. Spectral scaling in a tidal boundary layer. J. Phys. Oceanogr. **15**: 496–508, doi:10.1175/1520-0485(1985)015<0496:SSIATB>2.0.CO;2.

Hadfield, M. G., and M. A. R. Koehl. 2004. Rapid behavioral responses of an invertebrate larva to dissolved settlement cue. Biol. Bull. **207**: 28–43, doi:10.2307/1543626.

Hansen, B., F. L. Fotel, N. J. Jensen, and L. Wittrup. 1997. Physiological effects of the detergent linear alkylbenzene sulphonate on blue mussel larvae (*Mytilus edulis*) in laboratory and mesocosm experiments. Mar. Biol. **128**: 627–637, doi:10.1007/s002270050129.

Hopfinger, E. J., and J.-A. Toly. 1976. Spatially decaying turbulence and its relation to mixing across density interfaces. J. Fluid Mech. **78**: 155–175, doi:10.1017/S0022112076002371.

Hunt, H. L., and R. E. Scheibling. 1998. Spatial and temporal variability of patterns of colonization by mussels (*Mytilus trossulus, M. edulis*) on a wave-exposed rocky shore. Mar. Ecol. Prog. Ser. **167**: 155–169, doi:10.3354/meps167155.

Hwang, W., and J. K. Eaton. 2004. Creating homogeneous and isotropic turbulence without a mean flow. Exp. Fluids. **36**: 444–454, doi:10.1007/s00348-003-0742-6.

Jonsson, P. R., C. André, and M. Lindegarth. 1991. Swimming behaviour of marine bivalve larvae in a flume boundary-layer flow: Evidence for near-bottom confinement. Mar. Ecol. Prog. Ser. **79**: 67–76, doi:10.3354/meps079067.

Kingsford, M. J., J. M. Leis, A. Shanks, K. C. Lindeman, S. G. Morgan, and J. Pineda. 2002. Sensory environments, larval abilities and local self-recruitment. Bull. Mar. Sci. **70S**: 309–340.

Knights, A. M., T. P. Crowe, and G. Burnell. 2006. Mechanisms of larval transport: Vertical distribution of bivalve larvae varies with tidal conditions. Mar. Ecol. Prog. Ser. **326**: 167–174, doi:10.3354/meps326167.

Koehl, M. A. R., and M. A. Reidenbach. 2007. Swimming by microscopic organisms in ambient water flow. Exp. Fluids. **43**: 755–768, doi:10.1007/s00348-007-0371-6.

Koehl, M. A. R., J. A. Strother, M. A. Reidenbach, J. R. Koseff, and M. G. Hadfield. 2007. Individual-based model of larval transport to coral reefs in turbulent, wave-driven flow: Behavioral responses to dissolved settlement inducer. Mar. Ecol. Prog. Ser. **335**: 1–18, doi:10.3354/meps335001.

Lane, D. J. W., A. R. Beaumont, and J. R. Hunter. 1985. Byssus drifting and the drifting threads of the young post-larval mussel *Mytilus edulis*. Mar. Biol. **84**: 301–308, doi:10.1007/BF00392500.

Lazier, J. R. N., and K. H. Mann. 1989. Turbulence and the diffusive layers around small organisms. Deep-Sea Res. Part A. **36**: 1721–1733, doi:10.1016/0198-0149(89)90068-X.

Mackie, G. O., C. L. Singla, and C. Thiriot-Quievreux. 1976. Nervous control of ciliary activity in gastropod larvae. Biol. Bull. **151**: 182–199, doi:10.2307/1540713.

McCullagh, P., and J. A. Nelder. 1989. Generalized Linear Models. CRC Press.

McKenna, S. P. 2000. Free-surface turbulence and air-water gas exchange, PhD diss., MIT/Woods Hole Oceanographic Institution Joint Program.

McKenna, S. P., and W. R. McGillis. 2004. Observations of flow repeatability and secondary circulation in an oscillating grid-stirred tank. Phys. Fluids. **16**: 3499–3502, doi:10.1063/1.1779671.

McLachlan, G., and D. Peel. 2000. Finite Mixture Models. John Wiley and Sons.

Murakami, A., and K. Takahashi. 1975. Correlation of electrical and mechanical responses in nervous control of cilia. Nature. **257**: 48–49, doi:10.1038/257048a0.

North, E. W., Z. Schlag, R. R. Hood, M. Li, L. Zhong, T. Gross, and V. S. Kennedy. 2008. Vertical swimming behavior influences the dispersal of simulated oyster larvae in a coupled particle-tracking and hydrodynamic model of Chesapeake Bay. Mar. Ecol. Prog. Ser. **359**: 99–115, doi:10.3354/meps07317.

Oakey, N. S., and J. A. Elliott. 1982. Dissipation within the surface mixed layer. J. Phys. Oceanogr. **12**: 171–185, doi:10.1175/1520-0485(1982)012<0171:DWTSML>2.0.CO;2.

Pawlik, J., and C. A. Butman. 1993. Settlement of a marine tube worm as a function of current velocity: Interacting effects of hydrodynamics and behavior. Limnol. Oceanogr. **38**: 1730–1740, doi:10.4319/lo.1993.38.8.1730.

Peters, H. 1997. Observations of stratified turbulent mixing in an estuary: Neap-to-spring variations during high river flow. Estuar. Coast. Shelf Sci. **45**: 69–88, doi:10.1006/ecss.1996.0180.

Petersen, J. H. 1984. Larval settlement behavior in competing species: *Mytilus californianus* Conrad and *M. edulis* L. J. Exp. Mar. Biol. Ecol. **82**: 147–159, doi:10.1016/0022-0981(84)90100-X.

Pringle, J. M., and P. J. S. Franks. 2001. Asymmetric mixing transport: A horizontal transport mechanism for sinking plankton. Limnol. Oceanogr. **46**: 381–391, doi:10.4319/lo.2001.46.2.0381.

Raby, D., Y. Lagadeuc, J. J. Dodson, and M. Migelbier. 1994. Relationship between feeding and vertical distribution of bivalve larvae in stratified and mixed waters. Mar. Ecol. Prog. Ser. **103**: 275–284, doi:10.3354/meps103275.

Reeks, M. W. 1977. On the dispersion of small particles suspended in an isotropic turbulent fluid. J. Fluid Mech. **83**: 529–546, doi:10.1017/S0022112077001323.

Rothschild, B. J., and T. R. Osborn. 1988. Small-scale turbulence and plankton contact rates. J. Plankton Res. **10**: 465–474, doi:10.1093/plankt/10.3.465.

Saarenrinne, P., and M. Piirto. 2000. Turbulent kinetic energy dissipation rate estimation from PIV velocity vector fields. Exp. Fluids. **29**: S300–S307, doi:10.1007/s003480070032.

Shy, S. S., C. Y. Tang, and S. Y. Fann. 1997. A nearly isotropic turbulence generated by a pair of vibrating grids. Exp. Therm. Fluid Sci. **14**: 251–262, doi:10.1016/S0894-1777(96)00111-2.

Srdic, A., H. J. S. Fernando, and L. Montenegro. 1996. Generation of nearly isotropic turbulence using two oscillating grids. Exp. Fluids. **20**: 395–397, doi:10.1007/BF00191022.

Suchanek, T. H. 1978. The ecology of *Mytilus edulis* L. in exposed rocky intertidal communities. J. Exp. Mar. Biol. Ecol. **31**: 105–120, doi:10.1016/0022-0981(78)90139-9.

Tanaka, T., and J. K. Eaton. 2007. A correction method for measuring turbulence kinetic energy dissipation rate by PIV. Exp. Fluids. **42**: 893–902, doi:10.1007/s00348-007-0298-y.

Tennekes, H., and J. L. Lumley. 1972. A First Course in Turbulence. MIT Press.

Turner, E. J., R. K. Zimmer-Faust, M. A. Palmer, M. Luckenbach, and N. D. Pentcheff. 1994. Settlement of oyster (*Crassostrea virginica*) larvae: Effects of water flow and a water-soluble chemical cue. Limnol. Oceanogr. **39**: 1579–1593, doi:10.4319/lo.1994.39.7.1579.

Villermaux, E., B. Sixou, and Y. Gagne. 1995. Intense vortical structures in grid-generated turbulence. Phys. Fluids. **7**: 2008–2013, doi:10.1063/1.868512.

Webster, D. R., A. Brathwaite, and J. Yen. 2004. A novel laboratory apparatus for simulating isotropic oceanic turbulence at low Reynolds number. Limnol. Oceanogr. Methods. **2**: 1–12, doi:10.4319/lom.2004.2.1.

Welch, J. M., and R. B. J. Forward. 2001. Flood tide transport of blue crab, *Callinectes sapidus*, postlarvae: Behavioral responses to salinity and turbulence. Mar. Biol. **139**: 911–918, doi:10.1007/s002270100649.

Woodson, C. B., D. R. Webster, M. J. Weissbrg, and J. Yen. 2007. Cue hierarchy and foraging in calanoid copepods: Ecological implications of oceanographic structure. Mar. Ecol. Prog. Ser. **330**: 163–177, doi:10.3354/meps330163.

Yen, J., K. D. Rasberry, and D. R. Webster. 2008. Quantifying copepod kinematics in a laboratory turbulence apparatus. J. Mar. Syst. **69**: 283–294, doi:10.1016/j.jmarsys.2006.02.014.

Young, C. M. 1995. Behavior and locomotion during the dispersal phase of larval life. Pp. 249–278. *In* L. McEdward [ed.], Ecology of Marine Invertebrate Larvae. CRC Press.

Zucchini, W. 2000. An introduction to model selection. J. Math. Psychol. **44**: 41–61, doi:10.1006/jmps.1999.1276.

Received: 18 April 2011
Amended: 6 July 2011
Accepted: 22 July 2011